JOURNAL OF MATERIALS SCIENCE 31 (1996) 6279–6284

Thin hydroxyapatite layers formed on porous titanium using electrochemical and hydrothermal reaction

H. ISHIZAWA, M. OGINO
Biomedical Engineering Laboratory, Department of Technological Development, Nikon Corporation, 1-10-1 Asamizodai, Sagamihara-shi, Kanagawa 228, Japan

In our previous study, it was found that hydroxyapatite (HA) microcrystals were precipitated by hydrothermal treatment on an anodic titanium oxide film containing calcium and phosphorus (AOFCP) with an equivalent Ca/P ratio to HA, which was formed on a titanium metal anode in an aqueous electrolytic solution of dissolved calcium acetate and β-glycerophosphate. In this study, the formation mechanism of the AOFCP has been clarified. Spark discharges, which occur on titanium surface with a large amount of heat generation, cause crystallization of the TiO_2 matrix of the AOFCP and incorporation of calcium and phosphorus into the matrix from these electrolytes simultaneously. The calcium and phosphorus in the matrix seem to exist as ions rather than as calcium phosphate. Also, thin HA layers consisting of the many precipitated microcrystals can be uniformly formed even on titanium with complex shapes or surface geometries such as the mesh, roughened surfaces and bead-coated porous coating by the present method.

1. Introduction

Titanium implants have been clinically used for dental and orthopaedic applications owing to their good biocompatibility. Recently, hydroxyapatite (HA) coatings have been developed to obtain better compatibility with bone than titanium [1, 2]. In an early stage after implantation, HA-coated implants are surrounded by a large amount of newly formed bone, and establish firm fixation, because HA has the abilities to enhance the bone formation on itself and bond to bone directly. HA coatings have been commonly produced by a plasma-spraying technique. However, the HA coating has a few critical problems, such as easy dissolution or bioresorption in living tissue, and a potentially weak interfacial bond between the coating and a metal substrate [3, 4]. As a result, the low stability of the HA coating may lead to the failure of the implant.

Also, there is a technical problem that this method can offer uniform HA coatings only on implants whose shapes are relatively simple. HA powders are not deposited on inner or undercut surfaces of a porous structure. On the other hand, electrochemical processes essentially have a possibility that the whole surface of implants can be uniformly treated, even though their shapes or surface geometries are complex [5–8]. As regards this point, anodization of titanium may be a superior method among the processes, because the electrochemical reaction occurs wherever a titanium anode is in contact with an electrolytic solution. It also has the many advantages of easy operation, no need for special equipment, high reproducibility and high uniformity in film thickness. From a manufacturing point of view, it is expected to be one of the promising ways to prepare uniform bioactive material coatings for implants with complex shapes. So we have developed a new method for forming thin HA layers by means of electrochemical and hydrothermal reaction [9, 10]. First, an anodic titanium oxide film containing calcium and phosphorus (AOFCP) was formed by anodizing titanium in an electrolytic solution of dissolved sodium β-glycerophosphate (β-GP) and calcium acetate (CA) in water, and then heated at 300° C in high-pressure steam. As a result, a thin HA layer consisting of numerous HA mirocrystals precipitated on the AOFCP was synthesized. However, the electrochemical phenomena occurring on titanium during the anodization were not understood very well. The purpose of this study was to clarify the formation mechanism of the AOFCP. Also, an attempt was made, using this method, uniformly to form the thin HA layers on titanium substrates with rough or porous surfaces taking advantage of the fact that there is little restriction on implant shapes.

2. Experimental procedure

Commercially pure titanium was anodized in an electrolytic solution of dissolved β-GP and CA in distilled water. The anodization was performed up to 230 or 350 V using a regulated d.c. power supply, which

0022–2461

allowed automatic transition from constant current to constant voltage when a preset maximum voltage has been reached. Two types of electrolytic solutions with low (β-GP 0.04, CA 0.25 mol l^{-1}) and high (β-GP 0.12, CA 0.4 mol l^{-1}) electrolyte concentrations were used. The AOFCPs were formed slowly and rapidly at current densities of 10 and 50 mA cm^{-2}, and named 04-25S and 04-25R, and 12-4S and 12-4R, respectively. The electrolytic baths were kept at 20 °C by using cooling equipment. The surface microstructure of the film was observed by scanning electron microscopy (SEM; DS-130, Topcon). The atomic ratios of calcium and phosphorus to titanium (Ca/Ti and P/Ti ratio) were semi-quantitatively determined by an energy-dispersive X-ray microanalyser (EDX; PV9100, Philips). Data were acquired at an accelerating voltage of 15 kV for 100 s on the carbon-coated specimen. The crystal structure of the film was analysed by X-ray diffraction (XRD). Hydrothermal treatment was performed at 300 °C for 2 h in high-pressure steam using an autoclave (volume 1300 ml) in which 200 ml water was included. Titanium beads of 250–350 and 500–700 μm diameter were sintered on titanium substrates at 1150 °C in a vacuum. The porous coatings of the titanium beads with the single, double and triple layers were anodized and then hydrothermally heated.

3. Results

3.1. Titanium anodization in a solution containing CA and β-GP

Fig. 1 shows spark discharges occurring on a titanium rod in the electrolytic solution during the anodization. The occurrence started above about 200 V and nearly finished at the preset maximum voltage. It became more vigorous as the electrolytic voltage rose. The temperature of the electrolytic solution gradually rose during the anodization. For example, that of the solution of 200 ml rose from 10 °C to 35 °C during the anodization for forming 04-25R of 5.6 cm^2 area. Fig. 2 shows the surface microstructure of 04-25R. Many micropores were formed all over the film, corresponding to each occurrence of the spark discharge. There was no difference in surface microstructure between 04-25S and 04-25R. The time to finish the anodization was about 5 and 30 min for 04-25R and 04-25S, respectively. Therefore, the microstructure was hardly affected by the current density, that is, the formation rate of the film, when the electrolyte concentration was low. However, the effect of the formation rate on the microstructure became significant as the electrolyte concentration increased. The morphology of 12-4S was irregular as a whole, in comparison with 04-25S and 04-25R, although domains with regular microstructure, as seen for 04-25R in Fig. 2, partially remained (Fig. 3a). Furthermore, the area of the domain with each microstructure increased in the case of the rapidly formed 12-4R (Fig. 3b). The slowly formed AOFCP showed higher morphological uniformity in appearance, as well as microscopically, than the rapidly formed one when the electrolyte concentration was high.

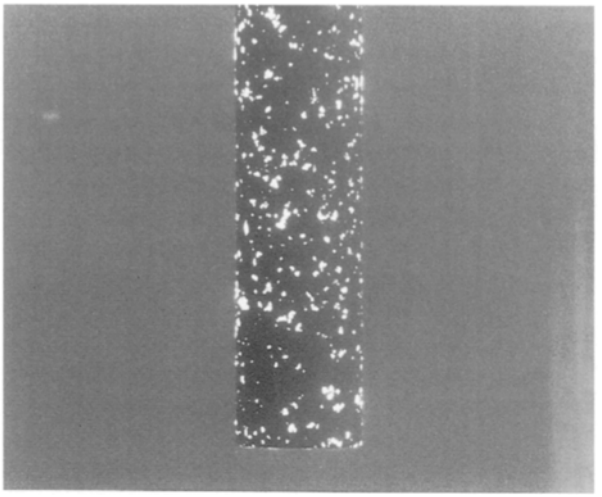

Figure 1 Spark discharges occurring on a titanium rod during the anodization.

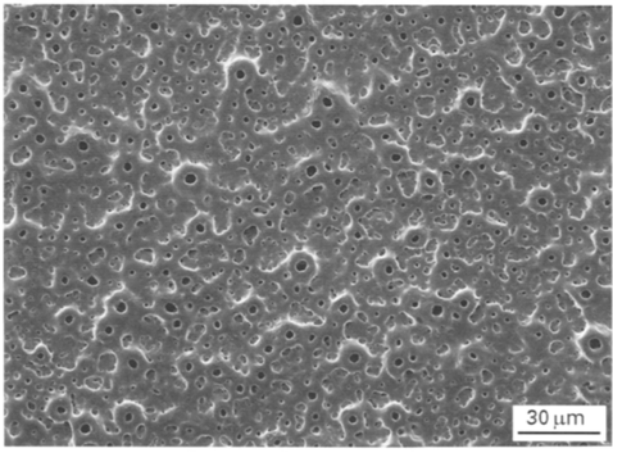

Figure 2 Scanning electron micrograph of 04-25R.

The variations in Ca/Ti and P/Ti ratios with CA concentration are shown in Fig. 4. The calcium and phosphorus contents in the AOFCP formed at β-GP of 0.12 mol l^{-1} were always much higher than those at 0.04 mol l^{-1}. The calcium content was not proportional to CA concentration. Although the β-GP concentration was constant at 0.04 or 0.12 mol l^{-1}, the phosphorus content varied with CA concentration. In particular, when β-GP concentration was 0.12 mol l^{-1}, there was an apparent correlation between these contents. The calcium and phosphorus in the AOFCP seemed to interact.

The X-ray diffraction patterns of 04-25S and 12-4S are shown in Fig. 5. 04-25S consisted of anatase and a little rutile phases, while 12-4S involved a trace of α-tricalcium phosphate as well as the same TiO_2 phases. The formation of HA was recognized for both hydrothermally treated AOFCPs (Fig. 6). 12-4S showed a slightly higher peak height of HA than 04-25S. From our previous studies, it is known that a thin HA layer of 1–2 μm thickness, which consists of the many precipitated crystals, is formed on the AOFCP by hydrothermal treatment [9, 10].

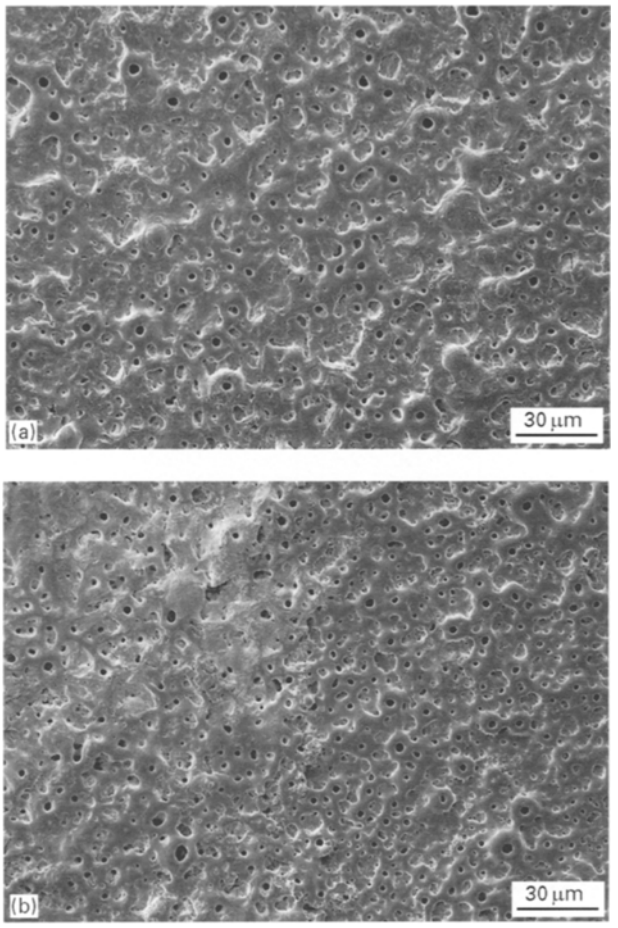

Figure 3 Scanning electron micrographs of (a) 12-4S and (b) 12-4R. Microdomains with regular or irregular microstructure were homogeneously dispersed in 12-4S. The area of the domain with each microstructure increased in 12-4S. In Fig. 3b, the right half had a regular microstructure and the left had an irregular one.

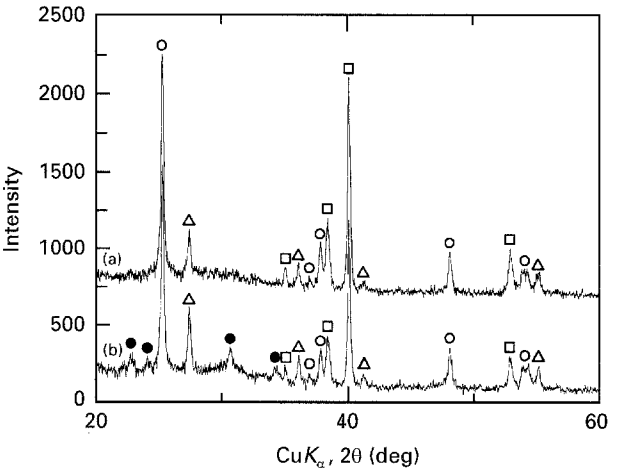

Figure 5 X-ray diffraction patterns of (a) 04-25S and (b) 12-4S (○) TiO_2 (anatase), (△) TiO_2 (rutile), (□) Ti (substrate), (●) α-tricalcium phosphate.

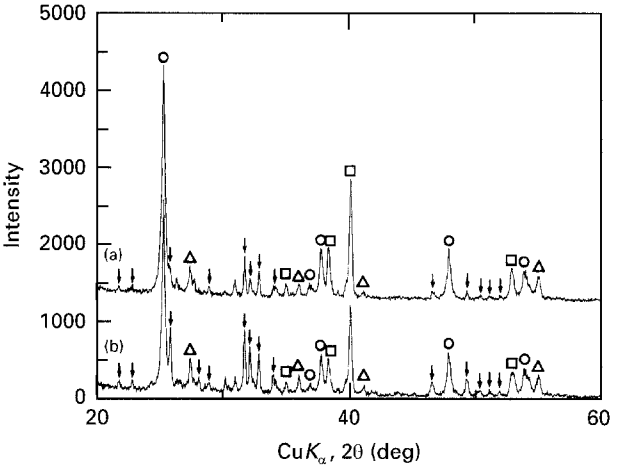

Figure 6 X-ray diffraction patterns of hydrothermally treated (a) 04-25S and (b) 12-4S. (○) TiO_2 (anatase), (△) TiO_2 (rutile), (□) Ti (substrate), (↓) HA.

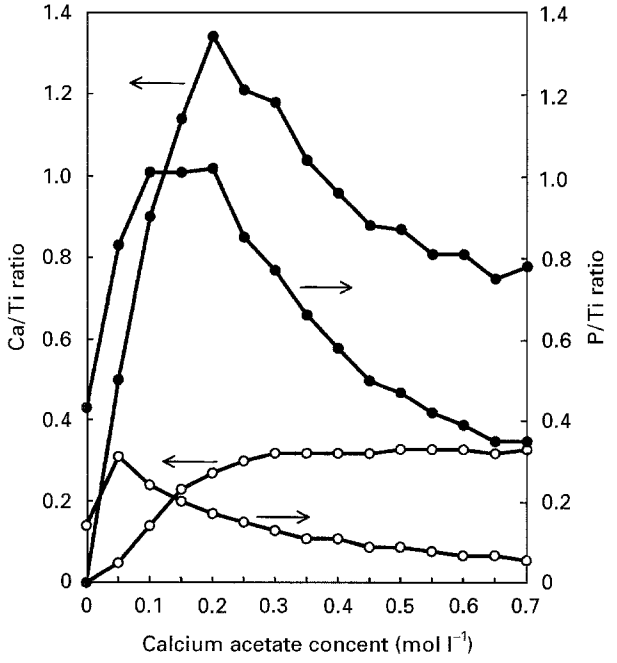

Figure 4 Variations of Ca/Ti and P/Ti ratios with CA concentration. The current density was 50 mA cm^{-2}. β-GP (mol l^{-1}): (○) 0.04, (●) 0.12.

3.2. Application of this method to titanium with various shapes

We applied this method to coat HA uniformly on titanium substrates with rough or porous surfaces. Such titanium substrates must be successfully anodized for the purpose, because the thin HA layer was always synthesized by hydrothermal treatment when the anodization was successful. Table I shows the results of the anodization for various titanium substrates with complex shapes. Grit-blasted and titanium plasma-sprayed surfaces were easily anodized under any anodization condition. However, if one does not want to diminish the surface roughness of the underlying substrate, the AOFCP would be as thin as possible, because the apparent surface roughness decreased with the result that the concavities were embedded in the thick AOFCP. The uniformly thin AOFCP was formed along the unevenly rough surface by lowering either the electrolyte concentration or the electrolytic voltage. After hydrothermal treatment, the AOFCP surface was covered with numerous precipitated HA crystals, as shown in Fig. 7a. Titanium mesh

TABLE I Results of anodization for various titanium with complex shapes

Titanium with complex shape	Concentration (mol l^{-1})		Voltage (V)	Result of anodization
	β-GP	CA		
Rough surface				
Grit-blasted surface	0.02	0.2	350	Good
Titanium plasma-sprayed surface	0.02	0.2	350	Good
Titanium mesh				
80 mesh cm^{-2}	0.02	0.2	350	Good
80 mesh cm^{-2}	0.06	0.3	350	Good
Titanium bead porous coating				
250–350 μm: single layer	0.06	0.4	230	Good
double layer	0.06	0.4	230	Good
triple layer	0.06	0.4	230	No good
500–700 μm: single layer	0.06	0.4	230	Good
double layer	0.06	0.4	230	Good
triple layer	0.06	0.4	230	No good

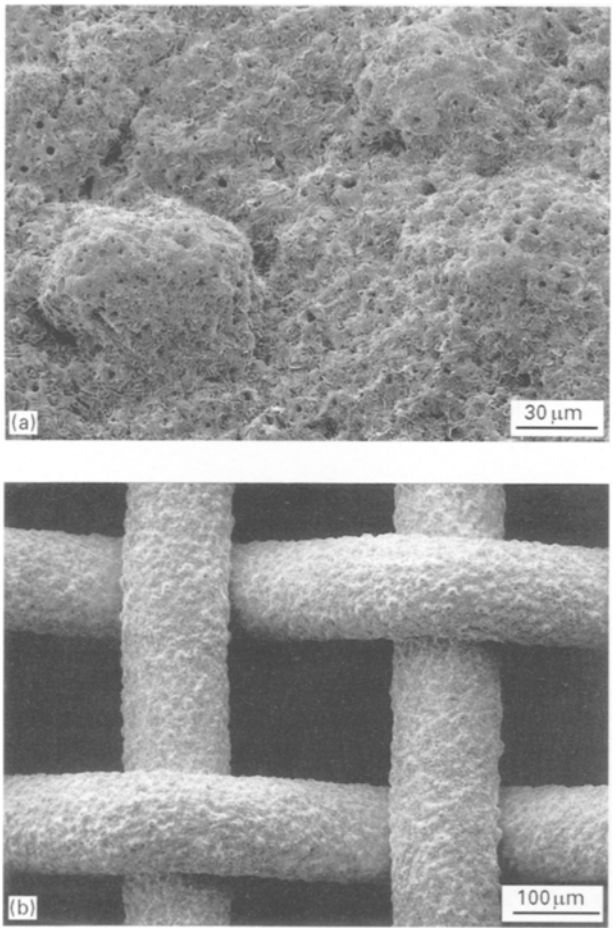

Figure 7 Scanning electron micrographs of anodized and then hydrothermally treated (a) titanium plasma-sprayed surface and (b) titanium mesh. These specimens were anodized up to 350 V at β-GP of 0.02 mol l^{-1} and CA of 0.2 mol l^{-1}.

was easily anodized, and the thin HA layer was uniformly synthesized over the whole surface (Fig. 7b). The anodization of titanium bead porous coatings was successful for single and double beads layers, but unsuccessful for the triple layers in the case of both bead diameters. It became more difficult to anodize stably such porous coatings with increasing number of the bead layers. Fig. 8a indicates that the AOFCP and the subsequent thin HA layer are successfully formed over the whole surface of the porous coating with double layers of beads of 250–350 μm diameter. It was confirmed that numerous precipitated HA crystals completely covered the bead surface situated even in the lower layer (Fig. 8c). However, the bottom surface of the porous coating was incompletely covered with the HA crystals (Fig. 8d). The thicknesses of the AOFCP and the thin HA layer were 10 and 2 μm at 350 V (β-GP 0.06, CA 0.3 mol l^{-1}), and 3 and 0.5 μm at 230 V (β-GP 0.06, CA 0.4 mol l^{-1}), respectively. The large decrease in film thickness caused by lowering the voltage enabled a uniform coating of HA which did not obstruct the narrow pores.

4. Discussion

4.1. Formation mechanism of the AOFCP

The increase in temperature of the electrolytic solution during the anodization suggests that the vigorous spark discharges generate a large amount of heat energy. Probably the AOFCP around every micropore is heated to a considerably high temperature the instant that the spark discharge occurs. Fig. 9 schematically shows the formation mechanism of the AOFCP by the spark discharge anodization. The spark discharges, which occur instantaneously at random points on titanium, as shown in Fig. 1, make the many micropores on the AOFCP. Usually, titanium is anodized using sulphuric acid, phosphoric acid or both, as electrolytes to obtain an anodic oxide film several micrometres thick. The oxide film consists of anatase and rutile phases crystallized by the high temperature of the spark discharge [11]. In the case of the anodization using β-GP and CA as electrolytes, incorporation of calcium and phosphorus from the electrolytes into the TiO_2 matrix of the AOFCP, as well as crystallization of the matrix, appear to occur simultaneously at every point where the spark discharge occurs. It is thought that the repetition of such electrochemical reaction results in the formation of the AOFCP. As the calcium and phosphorus contents in the matrix approach the limits, the homogeneous incorporation of calcium and phosphorus becomes

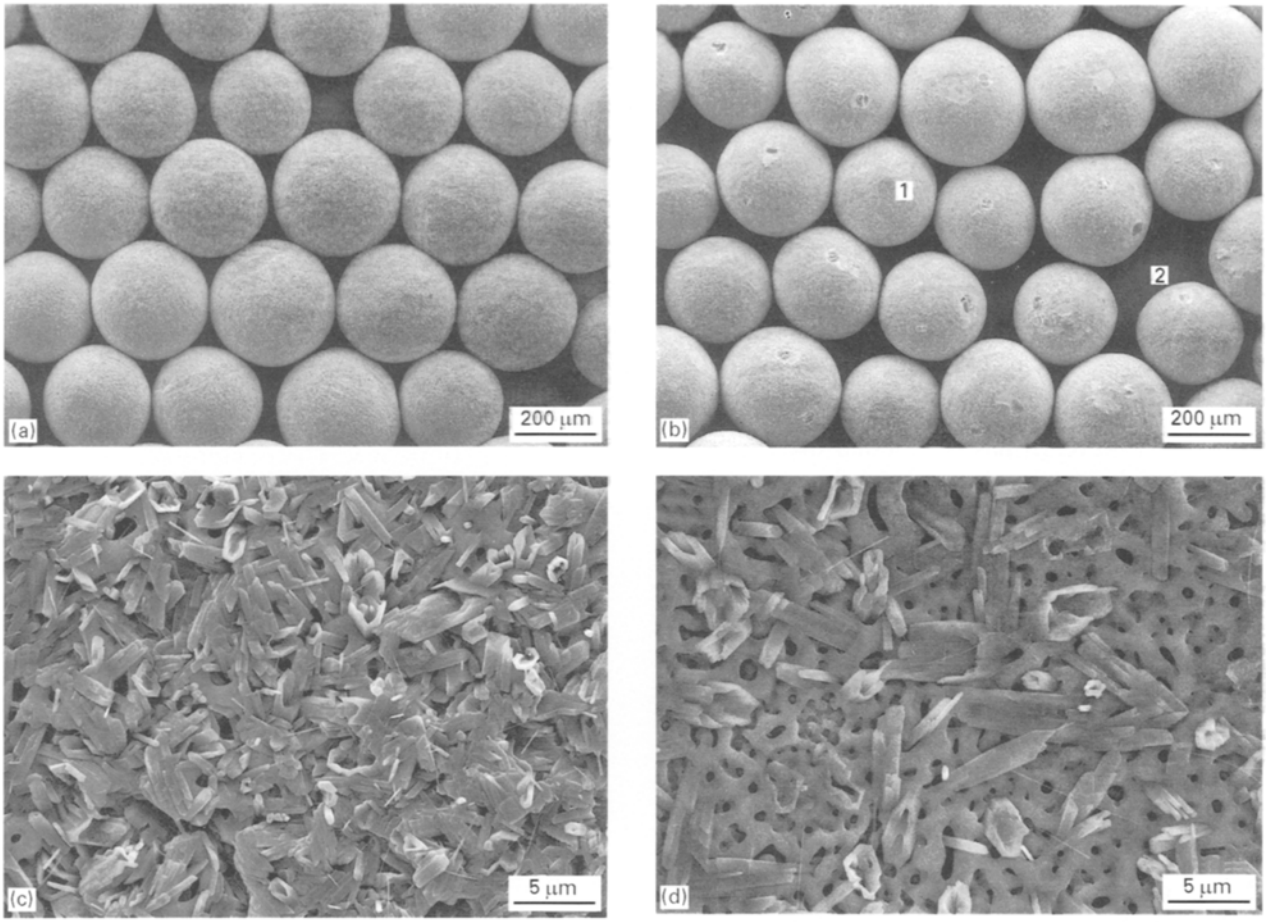

Figure 8 Scanning electron micrographs of anodized and then hydrothermally treated titanium bead porous coating with double bead layers. The bead diameter was 250–350 μm. (a) Overview of the as-prepared porous coating, (b) the lower layer exposed after eliminating the upper layer. Traces of the sinternecks between the adjacent beads were seen on each bead. (c, d) Highly magnified images of the points 1 (bead surface) and 2 (bottom surface) in (b), respectively.

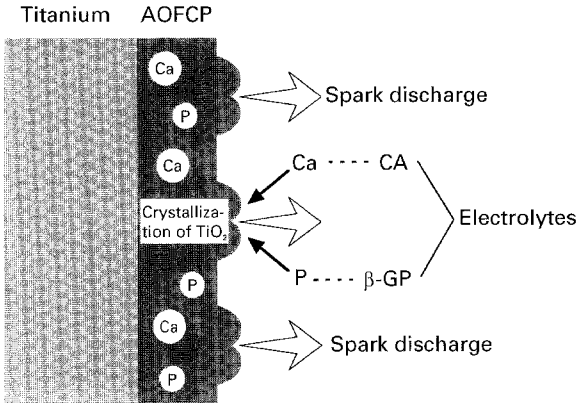

Figure 9 Schematic illustration showing the electrochemical formation process of the AOFCP by spark discharge anodization.

harder. Thus, it is necessary to perform the anodization as slowly as possible in that case.

It was obvious from Figs 4 and 5 that calcium and phosphorus existed in the AOFCP. However, no calcium phosphate peak was indicated in the XRD pattern for 04-25S. Most of the calcium and phosphorus in the AOFCP appears to exist not as calcium phosphate but as ions, although a trace of α-tricalcium phosphate is detected in 12-4S. The fact that calcium and phosphorus of which precipitated HA crystals consist are supplied only from the AOFCP, suggests that they are leached from the TiO_2 matrix and then crystallized to HA with hydroxyl groups in high-pressure steam.

4.2. Thin HA layer formation on titanium with rough or porous surface

It was not possible to anodize titanium bead porous coatings up to a high voltage of 350 V. As the AOFCP thickness increases with voltage, the pore size between the beads becomes narrow. Consequently, the circulation of the electrolytic solution through the porous coating deteriorates. Thus, the voltage has to be largely lowered from 350 V. As shown in Table I, the anodization of the porous coating at 230 V was successful for the single and double layers, but unsuccessful for the triple layers. The electrolyte concentration, as well as the voltage, must be changed to form the thin HA layer on the porous coating. Unless the electrolyte concentration is changed, the calcium and phosphorus contents in the AOFCP, and thus the amount of precipitation of HA will decrease due to the reduction in film thickness. As a consequence of the increase of CA concentration from 0.3 $mol\,l^{-1}$ to 0.4 $mol\,l^{-1}$, the thin AOFCP with sufficient calcium and phosphorus contents to precipitate numerous HA crystals, was formed at 230 V (Fig. 8a–c). This condition, with a low voltage and a high electrolyte concentration,

is also preferable to roughened titanium substrates such as grit-blasted and plasma-sprayed surfaces.

In fact, most implants have complex surface geometries or shapes to make the contact area with bone as large as possible. For example, stems and cups for total hip-joint replacement are often equipped over part of the surface with a titanium bead porous coating. In addition, some dental implants have surfaces roughened by grit-blasting or titanium plasma-spraying to obtain a mechanical interlocking force with bone, and/or are designed to be a complex shape, such as screw and blade. Many investigators have demonstrated that plasma-sprayed HA coatings enhance early bone ingrowth into metal bead porous coatings [12–14]. However, it has been found that a plasma-spraying technique is unsuitable for forming uniform HA coatings on the porous coating, because the relatively thick HA coating obstructs the narrow pores between the beads [15]. Thus, development of a coating method of HA which does not obstruct the pores is desired. The present method consists in the anodization of titanium and the subsequent hydrothermal treatment in high-pressure steam. Because these treatments are performed in liquid and vapour phases, respectively, it is essentially very advantageous to the uniform formation of the AOFCP and the thin HA layer. For this reason, a thin HA layer was uniformly synthesized on all the titanium beads, not obstructing the narrow pores. Another reason why this method makes the uniform HA coating possible is that the total film thickness of the AOFCP and the thin HA layer, is much thinner at 3.5 μm than that of a typical plasma-sprayed HA coating. Much bone ingrowth into the anodized and then hydrothermally treated porous titanium is expected by virtue of the osteoconductive property of the thin HA layer.

5. Conclusion

To make the thin HA layers on titanium implants, AOFCP was first made by anodizing titanium in an electrolytic solution containing β-GP and CA. The occurrence of the spark discharges played an important role in the formation of the AOFCP. The AOFCP should be formed as slowly as possible when the electrolyte concentration is high. The present method can offer uniform HA coatings on most implants, regardless of the shapes or surface geometries.

References

1. R. G. T. GEESINK, K. DE GROOT and C. P. A. T. KLEIN, *Clin. Orthop.* **225** (1987) 147.
2. S. D. COOK, K. A. THOMAS, J. F. KAY and M. JARCHO, *ibid.* **130** (1988) 303.
3. R. Y. WHITEHEAD, W. R. LACEFIELD and L. C. LUCAS, *J. Biomed. Mater. Res.* **27** (1993) 1501.
4. L. G. ELLIES, D. G. A. NELSON and J. D. B. FEATHERSTONE, *Biomaterials* **13** (1992) 313.
5. M. SHIRKHANZADEH, *J. Mater. Sci. Lett.* **10** (1991) 1415.
6. *Idem, J. Mater. Sci. Mater. Med.* **6** (1995) 90.
7. A. CIGADA, M. CABRINI and P. PEDEFERRI, *ibid.* **3** (1992) 408.
8. P. DUCHEYNE, S. RADIN, M. HEUGHEBAERT and J. C. HEUGHEBAERT, *Biomaterials* **11** (1990) 244.
9. H. ISHIZAWA and M. OGINO, *J. Biomed. Mater. Res.* **29** (1995) 65.
10. *Idem, ibid.* **29** (1995) 1071.
11. S. ITO, K. KOIZUKA, M. HIROCHI, T. ONAKA, H. MATSUNAGA and T. HANADA, *Shikizai* **61** (1988) 599.
12. H. OONISHI, T. NODA, S. ITO, A. KOHDA, H. ISHIMARU, M. YAMAMOTO and E. TSUJI, *J. Appl. Biomater.* **5** (1994) 23.
13. A. MORONI, V. L. CAJA, E. L. EGGER, L. TRINCHESE and E. Y. S. CHAO, *Biomaterials* **15** (1994) 926.
14. S. D. COOK, K. A. THOMAS, L. E. DALTON, T. K. VOLKMAN, T. S. WHITECLOUD III and J. F. KAY, *J. Biomed. Mater. Reš.* **26** (1992) 989.
15. K. HAYASHI, T. INADOME, H. TSUMURA, Y. NAKASHIMA and Y. SUGIOKA, *Biomaterials* **15** (1994) 1187.

Received 9 May 1995
and accepted 2 July 1996